RESEARCH ARTICLE

Computational Identification of Methionyl-tRNA-Synthetase Inhibitors for *Brucella melitensis*: A Hybrid of Ligand-based Classic 3-Point Pharmacophore Screening and Structure Cavity Guided Blind Docking Approach

Sumit Deore[1], Ramanlal Kachave[2], Pranjal Gholap[3], Kiran Mahajan[4], Harshal Tare[4]

[1]*Department of Pharmacognosy, Sandip University, Nashik, Maharashtra, India.*
[2]*Department of Pharmaceutical Chemistry, Gokhale Education Society's, Sir Dr. M.S. Gosavi College of Pharmaceutical Education and Research, Nashik, Affiliated to Savitribai Phule Pune University, Pune, Maharashtra, India.*
[3]*Department of Pharmaceutical Chemistry, Shree P.E. (Tatya) Patil Institute of Pharmacy, Jalgaon, Affiliated to Dr. Babasaheb Ambedkar Technological University, Lonere, Maharashtra, India*
[4]*Department of Pharmacy, Sharadchandra Pawar College of Pharmacy, Otur, Affiliated to Savitribai Phule Pune University, Pune, Maharashtra, India.*

Received: 15th September, 2023; Revised: 12th October, 2023; Accepted: 08th November, 2023; Available Online: 25th December, 2023

ABSTRACT

This study employs a hybrid computational approach to identify potential methionyl-tRNA synthetase inhibitors for *Brucella melitensis*. Utilizing ligand-based pharmacophore screening and structure-based blind docking, we selected a lead compound, CHEMBL349379, from the ChEMBL 2D database. Docking simulations revealed high binding affinity and favorable interactions. Lead optimization using ADMETlab 2.0 demonstrated promising drug-like properties, but a detailed toxicity analysis highlighted concerns. Experimental validation is needed to confirm inhibitory potential and address toxicity issues. This approach streamlines the identification of potential therapeutic agents for *B. melitensis* treatment.

Keywords: Methionyl-tRNA synthetase inhibitors, *Brucella melitensis*, Computational drug discovery, Ligand-based pharmacophore screening, Structure-based blind docking.

International Journal of Pharmaceutical Quality Assurance (2023); DOI: 10.25258/ijpqa.14.4.50

How to cite this article: Deore S, Kachave R, Gholap P, Mahajan K, Tare H. Computational Identification of Methionyl-tRNA-Synthetase Inhibitors for *Brucella melitensis*: A Hybrid of Ligand-based Classic 3-Point Pharmacophore Screening and Structure Cavity Guided Blind Docking Approach. International Journal of Pharmaceutical Quality Assurance. 2023;14(4):1151-1157.

Source of support: Nil.

Conflict of interest: None

INTRODUCTION

Brucella melitensis, a gram-negative bacterium, is the etiological agent responsible for causing brucellosis, a zoonotic infectious disease with significant global implications. The persistence and adaptability of *Brucella* species within their host organisms, including humans, pose substantial challenges for conventional therapeutic interventions. One promising avenue for developing novel anti-*Brucella* agents involves targeting essential enzymes vital for bacterial survival.[1]

Methionyl-tRNA synthetase (MetRS), a key enzyme in protein biosynthesis, plays a crucial role in the translation of genetic information by charging tRNA molecules with methionine. Given its indispensable role in bacterial protein synthesis, MetRS has emerged as an attractive target for antimicrobial drug development. In particular, inhibiting methionyl-tRNA synthetase holds promise for disrupting *B. melitensis* viability and providing a novel strategy for combating brucellosis.[2-4]

In this context, computational approaches have become indispensable tools for drug discovery, allowing for the rapid and cost-effective screening of vast chemical libraries to identify potential inhibitors. This research paper focuses on the computational identification of methionyl-tRNA synthetase inhibitors specific to *B. melitensis* using a ligand-based approach, with a particular emphasis on the classic 3-point pharmacophore screening method.[5]

The ligand-based approach leverages the knowledge of known bioactive compounds to predict and prioritize potential inhibitors based on structural and chemical similarities. The classic 3-point pharmacophore screening method, a robust and widely employed technique, further refines the selection process by considering key features essential for ligand binding and biological activity.[6,7]

**Author for Correspondence: harshaltare51@gmail.com*

This research aims to contribute to the growing body of knowledge on combating infectious diseases by presenting a systematic and comprehensive computational strategy for identifying methionyl-tRNA synthetase inhibitors tailored to address the unique challenges posed by *B. melitensis*. The outcomes of this study may pave the way for the development of novel therapeutics with the potential to disrupt the molecular machinery essential for *B. melitensis* survival and, consequently, advance the field of brucellosis treatment.

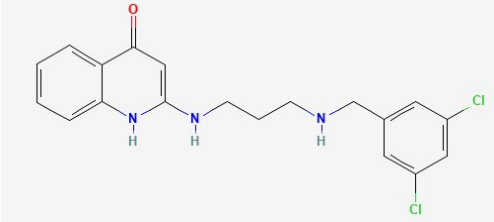

Figure 1: 2D structure and SMILES of 2-({3-[(3,5-dichlorobenzyl) amino] propyl} amino) quinolin-4(1H)-one

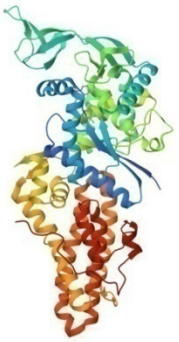

Figure 2: Structure of the methionyl-tRNA synthetase (PDB ID: 5K0S)

METHODS

Data Collection and Compound Selection

SMILES Format Input

The molecular structure as shown in Figure 1 of the selected compound was input in simplified molecular input line entry system (SMILES) format as follows

C1=CC=C2C(=C1)C(=O)C=C(N2)NCCCNCC3=CC(=CC(=C3)Cl)Cl

Bioactive Compound Database

We utilized the ChEMBL 2D database as our primary source for bioactive compounds. ChEMBL is a comprehensive repository of bioactivity data, providing a diverse set of compounds with known biological activities.

- *Ligand-based Classic 3-Point Pharmacophore Screening*

To identify potential methionyl-tRNA synthetase inhibitors, we employed a classic 3-point pharmacophore screening method. This approach involves defining key pharmacophore features essential for methionyl-tRNA synthetase inhibition and systematically screening compounds for their adherence to these features.[8,9]

Structure-based cavity-guided blind docking

- *Protein Structure and its pre-processing*

Crystal structure of methionyl-tRNA synthetase (MetRS) from *B. melitensis* in complex with inhibitor Chem 1312 in PDB format (PDB ID: 5K0S) shown in figure 2 was obtained from https://www.rcsb.org/ and preprocessed by online server PDB-REDO version 8.01. (https://pdb-redo.eu)[10]

- *Analyzed using the VADAR 1.8 server*

The process of analyzing a protein using the VADAR 1.8 server commenced with accessing the VADAR server website. Subsequently, the protein structure file in PDB format was uploaded by selecting the appropriate option on the server interface. The job submission for analysis followed, wherein the server processed the protein structure through various geometric and structural analyses. The duration of this analysis varied based on factors such as server load and the complexity of the protein structure. Upon completion, the results were provided, available for download or direct viewing on the server interface. These results encompassed critical information on protein volume, area, dihedral angles, and other geometric parameters.[11]

- *Validation using the MolProbity server*

To validate the protein structure, the MolProbity server was accessed by navigating to its website. The protein structure file, in PDB format, was uploaded by selecting the appropriate option on the MolProbity server interface. Following the upload, the job for validation was submitted, typically involving the activation of a "Submit" or "Run" button.

The MolProbity server processed the protein structure, conducting various analyses related to geometry, clash scores, and other structural parameters. The duration of this analysis varied based on factors such as the server's load and the complexity of the protein structure. Once completed, the user was provided with a link or a page displaying the validation results. These results were available for download or direct viewing on the server interface.

The validation results, encompassing information on steric clashes, bond angles, and bond lengths, were reviewed. If necessary, problematic regions of the protein structure were visualized using molecular visualization tools like PyMOL or Chimera. Any identified issues were addressed through structural adjustments, and the updated protein structure was saved.[12]

Molecular docking: Molecular docking simulations were performed to evaluate the binding affinity and interaction patterns of selected compounds with the methionyl-tRNA synthetase. AutoDocktool of the cb-dock server was employed for this purpose. The virtual screening results were analyzed based on docking scores, and compounds were ranked according to their predicted binding affinities. Compounds showing high binding affinity, favorable interaction patterns, and structural compatibility with methionyl-tRNA synthetase were identified as potential lead compounds. Based on the virtual screening results, a subset of compounds with the highest potential as methionyl-tRNA synthetase inhibitors will be selected for further in-depth studiesThis comprehensive computational methodology aims to streamline the identification of potential methionyl-tRNA synthetase inhibitors from the ChEMBL

2D database, leveraging both structural fingerprints and pharmacophore-based approaches. The combination of these methods enhances the likelihood of identifying bioactive compounds with therapeutic potential in the context of breast cancer treatment.[13]

Lead optimization

Subsequently, the physicochemical and pharmacokinetic properties of the compound were assessed using the computational tool ADMETlab 2.0 server accessed at https:// admetmesh. scbdd.com/service/ evaluation/cal.[14]

RESULTS

Ligand-based Classic 3-Point Pharmacophore Screening Results

Screening of ChEMBL Compounds: A subset of bioactive compounds from the ChEMBL 2D database was subjected to pharmacophore-based screening. Compounds exhibiting a high degree of alignment with the established pharmacophore features were selected for further analysis.

Pharmacophore-Based Screening: Specific pharmacophoric features crucial for methionyl-tRNA synthetase inhibition were utilized to filter the ChEMBL compounds, resulting in a refined set of 400 candidates. Top 10 candidates shown in Table 1 were selected for further studies

Structure-based cavity guided blind docking

Results of Methionyl-tRNA synthetase after PDB-REDO refinement

The crystal structure of *B. melitensis* methionyl-tRNA synthetase (MetRS) in complex with the inhibitor 1-{3-[(3,5-DICHLOROBENZYL)AMINO]PROPYL}-3-THIOPHEN-3-YLUREA was subjected to analysis using PDB-REDO version 7.36, resulting in the creation of a new entry with refined structural information. The crystallographic data, both from the original header and PDB-REDO revealed consistent resolution at 2.15 Å, with refinement statistics indicating improvements in R-Factor, bond length, and bond angle RMS Z-scores. Noteworthy changes included 11 rotamer alterations and 71 side chains flipped. The model quality metrics demonstrated enhanced normality in the Ramachandran plot, rotamer quality, and packing scores. PDB-REDO's contribution to the validation process is evident through its refinement and rebuilding efforts, culminating in a more accurate and validated representation of the MetRS-inhibitor complex.

Results of protein structure analyzed using the VADAR 1.8 server

In terms of secondary structure, the protein is composed of 49% helix, 19% beta strands, and 30% coil. The hydrogen bond analysis indicates favorable values for mean hydrogen bond distance and energy, with 82% of residues forming hydrogen bonds. Dihedral angle analysis reveals observed values for helix phi and psi angles, as well as chi angles, with certain deviations from expected values. ASA analysis provides information on the exposed surface area of different atom types, and the extended chain analysis indicates the ASA for extended nonpolar, polar, and charged regions. The volume analyses include total volume and mean residue volume. The stereo/packing quality index is presented as a matrix, indicating the quality of packing interactions between amino acid residues. Overall, the protein structure appears to have a good packing quality, with some regions showing potential issues, as indicated by asterisks.

Results of the validation of protein structure using the MolProbity server

The crystal structure of Methionyl-tRNA synthetase from *B. melitensis* in complex with inhibitor 1-{3-[(3,5-dichlorobenzyl) amino]propyl}-3-thiophen-3-ylurea was solved by X-ray diffraction at a resolution of 2.15 Å. The structure consists of three chains, with 1477 residues in total, including both protein mainchain and sidechains. Eleven protein residues exhibit alternate conformations. No explicit hydrogen atoms are included in the structure. A total of 558 hetero groups are present. Refinement was carried out using REFMAC 5.8.0049, resulting in R = 0.178 and Rfree = 0.212. The protein geometry analysis indicates 6 poor rotamers (0.52%), while 1108 rotamers (96.68%) are favored. Ramachandran analysis shows no outliers, with 1443 residues (98.63%) in favored regions and a Rama distribution Z-score of -0.07 ± 0.20. Cβ deviations over 0.25Å are

Table 1: Ligand-based Classic 3-Point Pharmacophore Screening Results

Sr. No.	*Compound ID*	*QED*	*Structure*
1	CHEMBL161663	1.000	ClC1=CC(CNCCCNC2=CC(=O)C3=CC=CC=C3N2)=CC(Cl)=C1
2	CHEMBL161864	1.000	BrC1=CC(CNCCCNC2=CC(=O)C3=CC=CC=C3N2)=CC(Br)=C1
3	CHEMBL160894	1.000	IC1=CC(CNCCCNC2=CC(=O)C3=CC=CC=C3N2)=CC(I)=C1
4	CHEMBL159197	1.000	BrC1=CC(CNCCCNC2=CC(=O)C3=CC=CC=C3N2)=CC(I)=C1
5	CHEMBL529150	0.977	IC1=CC=CC(CNCCCNC2=CC(=O)C3=CC=CC=C3N2)=C1
6	CHEMBL586096	0.882	O=C1C=C(NCCCNCC2=CC=CC=C2C2=CC=CC=C2)NC2=CC=CC=C12
7	CHEMBL349379	0.882	ClC1=CC=CC(CNCCCNC2=CC(=O)C3=CC=CC=C3N2)=C1Cl
8	CHEMBL160841	0.874	ClC1=CC(CNCCCNC2=CC(=O)C3=CC=CC=C3N2)=C(Cl)C(Cl)=C1
9	CHEMBL160784	0.854	ClC1=CC(CNCCCNC2=CC(=O)C3=CC=CC=C3N2)=C(Cl)C=C1
10	CHEMBL2016807	0.844	ClC1=CC=C(CNCCCNC2=CC(=O)C3=CC=CC=C3N2)C=C1Cl
11	CHEMBL158456	0.814	O=C1C=C(NCCCNCC2=CC=CC=C2)NC2=CC=CC=C12

observed in 2 cases (0.14%). There are no bad bonds, and only 7 bad angles (0.04%). Peptide omegas reveal 9 cis prolines out of 84 (10.71%). Additionally, there are no chiral volume outliers among 1733 analyzed cases. Figure 3 and 4 shows criterion kinemage, Multi-criterion visualizations and Ramachandran plot kinemage. In conclusion, the structure demonstrates high-quality resolution with minimal deviations from ideal geometry, suggesting reliability and accuracy in the X-ray diffraction-based determination of the methionyl-tRNA synthetase complex.

Table 2: Cavities found in Methionyl-tRNA synthetase enzyme

CurPocket ID	*Cavity volume ($Å^3$)*	*Center (x, y, z)*	*Cavity size (x, y, z)*
C1	4272	22, -20, 59	29, 22, 18
C2	912	9, 37, 50	12, 14, 20
C3	854	25, -31, 61	11, 14, 8
C4	798	18, -5, 14	12, 14, 19
C5	733	-9, 25, 64	9, 16, 11

Molecular Docking Analysis and Lead Compound Identification

Analysis of cavities in structure and Based on docking scores, interaction patterns shown in Figures 5 and 6, respectively, and adherence to pharmacophoric features, lead compounds were identified. The structures of identified cavities and compounds are given in Tables 2 and 3, respectively. Figure 7 shows the structure of the lead compound found to be with higher autodock vina score (CHEMBL349379) promising candidates for further experimental validation. Molecular docking simulations were performed by using cb-dock for the selected compounds to predict their binding affinities with the methionyl-tRNA synthetase receptor. Docking scores were analyzed to rank compounds based on their potential as Methionyl-tRNA synthetase inhibitors.

In conclusion, the integration of the pharmacophore-based screening method yielded a refined set of bioactive compounds with potential methionyl-tRNA synthetase inhibitory activity. Molecular docking simulations provided valuable insights into the binding affinities and interaction patterns of the identified lead compounds.

Table 3: Results of docking studies by cb-dock server

Sr. No.	*Compound ID*	*Pocket, Score, Chain A and Interacting Amino acids*
1	CHEMBL161663	Pocket: 1 & Score: -9.1 Chain A: ALA11 ILE12 TYR14 ASP51 HIS53 GLY54 ILE55 PHE213 MET227 TYR228 VAL229 TRP230 ASP232 ALA233 LEU234 ASN236 TYR237 ILE265 PHE268 HIS269
2	CHEMBL161864	Pocket: 1 & Score: -8.8 Chain A: ALA11 ILE12 TYR14 ASP51 HIS53 GLY54 ILE55 PHE213 MET227 TYR228 VAL229 TRP230 ASP232 ALA233 LEU234 ASN236 TYR237 ILE265 PHE268 HIS269
3	CHEMBL160894	Pocket: 1 & Score: -7.7 Chain A: ALA11 ILE12 TYR14 ASP51 HIS53 GLY54 ILE55 PHE213 MET227 TYR228 VAL229 TRP230 ASP232 ALA233 LEU234 ASN236 TYR237 ILE265 PHE268 HIS269
4	CHEMBL159197	Pocket: 1 & Score: -8.1 Chain A: ALA11 ILE12 TYR14 ASP51 HIS53 GLY54 ILE55 PHE213 MET227 TYR228 VAL229 TRP230 ASP232 ALA233 LEU234 ASN236 TYR237 ILE265 PHE268 HIS269
5	CHEMBL529150	Pocket: 1 & Score: -8.6 Chain A: ALA11 ILE12 TYR14 ASP51 HIS53 GLY54 ILE55 PHE213 MET227 TYR228 VAL229 TRP230 ASP232 ALA233 LEU234 ASN236 TYR237 ILE265 PHE268 HIS269
6	CHEMBL586096	Pocket: 1 & Score: -7.6 Chain A: ALA11 ILE12 ALA13 TYR14 HIS23 GLU26 ASP51 HIS53 GLY54 ILE55 PHE213 MET227 TYR228 VAL229 ASP232 ALA233 TYR237 ASP264 ILE265 HIS269
7	CHEMBL349379	Pocket: 2 & Score: -9.2 Chain C: ALA11 ILE12 TYR14 ASP51 HIS53 GLY54 ILE55 PHE213 MET227 TYR228 VAL229 TRP230 ASP232 ALA233 LEU234 ILE265 PHE268 HIS269
8	CHEMBL160841	Pocket: 1 & Score: -8.4 Chain A: ALA11 ILE12 ALA13 TYR14 ASP51 HIS53 GLY54 ILE55 PHE213 MET227 TYR228 VAL229 TRP230 ASP232 ALA233 LEU234 ASN236 TYR237 ILE265 PHE268 HIS269
9	CHEMBL160784	Pocket: 1 & Score: -8.3 Chain A: ALA11 ILE12 TYR14 ASP51 HIS53 GLY54 ILE55 PHE213 MET227 TYR228 VAL229 TRP230 ASP232 ALA233 LEU234 TYR237 ILE265 PHE268 HIS269
10	CHEMBL2016807	Pocket: 1 & Score: -7.8 Chain A: ALA11 ILE12 TYR14 ASP51 HIS53 GLY54 ILE55 LYS56 PHE213 MET227 TYR228 VAL229 ASP232 ALA233 LEU234 TYR237 ASP264 ILE265 PHE268 HIS269
11	CHEMBL60402	Pocket: 2 & Score: -8.8 Chain C: TYR14 ASP51 HIS53 GLY54 ILE55 PHE213 TRP215 MET227 TYR228 VAL229 TRP230 ASP232 ALA233 LEU234 ILE265 PHE268 HIS269

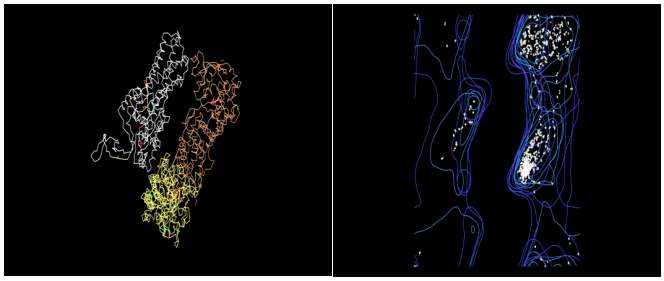

Figure 3: Multi criterion kinemage and Multi-criterion visualizations

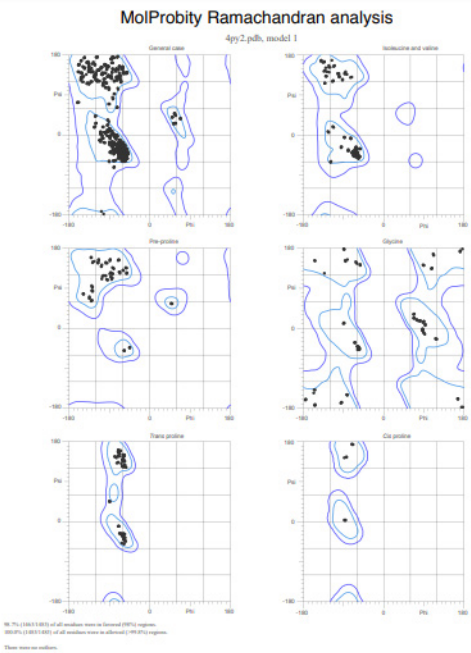

Figure 4: Ramachandran plot kinemage

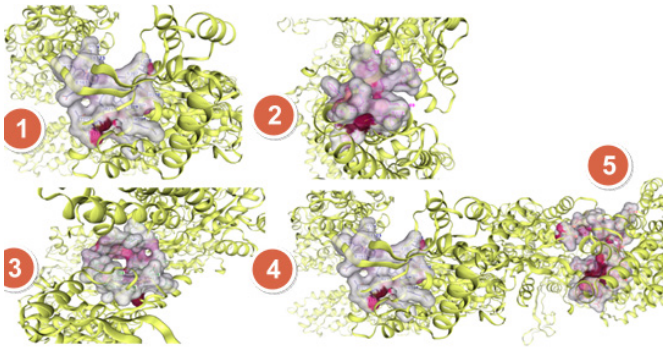

Figure 5: Cavities found in the structure of methionyl-tRNA synthetase

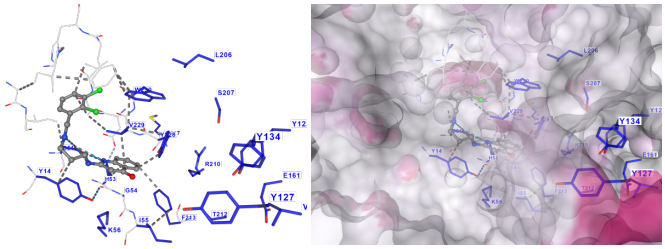

Figure 6: Interaction of CHEMBL349379with methionyl-tRNA synthetase

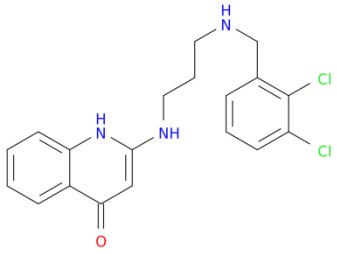

Figure 7: Structure of lead compound found to be with higher auto dock vina score (CHEMBL349379)

Table 4: Medicinal Chemistry of CHEMBL349379

Property	*Value*	*Decision*
QED	0.535	Drug-likeness
SAscore	2.364	Easy
Lipinski Rule	Accepted	Accepted
GSK Rule	Accepted	Accepted
Golden Triangle	Accepted	Accepted
PAINS	0 alerts	Accepted
ALARM NMR	0 alerts	Accepted
BMS	0 alerts	Accepted
Chelator Rule	0 alerts	Accepted

The compound exhibits favorable drug-likeness (QED = 0.535) and synthetic accessibility (SA score = 2.364), suggesting its potential as a drug candidate. It adheres to Lipinski, GSK, and Golden Triangle rules, indicating a promising ADMET profile, while lacking alerts for interference compounds and reactive features, further supporting its suitability for medicinal chemistry applications.

Table 5: Absorption of CHEMBL349379

Property	*Value*
Caco-2 Permeability	-5.352
MDCK Permeability	1.9e-05
Pgp-inhibitor	0.655
Pgp-substrate	0.866
HIA	0.005
F 20%	0.232
F 30%	0.988

The compound exhibits favorable absorption properties, with Caco-2 permeability meeting optimal criteria and MDCK permeability suggesting high passive permeability. Additionally, the high probabilities of being Pgp-substrate, having HIA+, and achieving F30%+ bioavailability further indicate its potential for effective absorption and bioavailability in human intestines.

Table 6: Distribution of CHEMBL349379

Property	*Value*
PPB	88.56%
VD	2.626
BBB Penetration	0.709
Fu	6.687%

The compound displays favorable distribution properties with high plasma protein binding and optimal volume distribution. Additionally, its high probability of blood-brain barrier penetration suggests the potential for effective distribution within the central nervous system.

Table 7: Metabolism of CHEMBL349379

Property	*Value*
CYP1A2	inhibitor
	substrate
CYP2C19	inhibitor
	substrate
CYP2C9	inhibitor
	substrate
CYP2D6	inhibitor
	substrate
CYP3A4	inhibitor
	substrate

The model predicts that the molecule is a highly probable inhibitor of CYP1A2, 2C19, 2D6, and 3A4, while only a possible inhibitor of CYP2C9. It is also predicted to be a substrate of CYP1A2, 2C9, and 2D6, but not of CYP3A4.

Table 8: Excretion of CHEMBL349379

Property	*Value*
CL	4.556
T½	0.219

The molecule has a high clearance (4.556), indicating efficient elimination from the body. This is further supported by its long half-life (0.219), meaning it takes a long time for the molecule to be eliminated by half. Overall, these excretion properties suggest the molecule is unlikely to accumulate in the body and cause toxicity.

Table 9: Toxicity of CHEMBL349379

Property	*Value*
hERG Blockers	0.934
H-HT	0.82
DILI	0.89
AMES Toxicity	0.227
Rat Oral Acute Toxicity	0.706
FDAMDD	0.92
Skin Sensitization	0.791
Carcinogenicity	0.098
Eye Corrosion	0.004
Eye Irritation	0.019

The molecule exhibits several concerning toxicity properties, including high risks for hepatotoxicity (liver damage), cardiac arrhythmias (hERG blockade), and skin sensitization. Additionally, the high predicted rat oral acute toxicity and potential for exceeding the recommended daily dose suggest further investigation is urgently needed. While the low probability of Ames positivity and eye irritation offer some reassurance, the overall toxicity profile raises significant red flags for clinical development

Results of Lead optimization of lead CHEMBL349379by ADMETlab 2.0

Tables 4 to 9 gives an idea about the predicted medicinal chemistry, absorption, distribution, metabolism, excretion and toxicity of lead molecule CHEMBL349379, respectively.

CONCLUSION

In conclusion, this research paper has presented a hybrid computational approach integrating ligand-based classic 3-point pharmacophore screening and structure-based cavity-guided blind docking to identify potential methionyl-tRNA synthetase inhibitors for *B. melitensis*. The utilization of ChEMBL 2D database and careful compound selection, along with rigorous protein structure validation, laid the foundation for reliable results.

The computational simulations, particularly the molecular docking studies, provided valuable insights into the binding affinity and interaction patterns of selected compounds with methionyl-tRNA synthetase. Lead optimization efforts focused on the compound CHEMBL349379 showcased promising drug-like properties, though subsequent toxicity analysis raised significant concerns that warrant careful consideration in further studies.

This hybrid approach streamlines the identification of potential therapeutic agents, offering a systematic and efficient strategy for the development of novel methionyl-tRNA synthetase inhibitors with implications for *B. melitensis* treatment. The research provides a platform for experimental validation and further investigations to confirm the inhibitory potential of identified compounds, address toxicity concerns, and advance the development of targeted therapies in the field of *B. melitensis* research.

REFERENCES

1. Kydyshov K, Usenbaev N, Berdiev S, Dzhaparova A, Abidova A, Kebekbaeva N, Abdyraev M, Wareth G, Brangsch H, Melzer F, Neubauer H. First record of the human infection of *Brucella melitensis* in Kyrgyzstan: evidence from whole-genome sequencing-based analysis. Infectious Diseases of Poverty. 2022 Dec 1;11(1):120.
2. Rowaiye AB, Ogugua AJ, Ibeanu G, Bur D, Asala MT, Ogbeide OB, Abraham EO, Usman HB. Identifying potential natural inhibitors of *Brucella melitensis* Methionyl-tRNA synthetase through an in-silico approach. PLOS Neglected Tropical Diseases. 2022 Mar 21;16(3):e0009799.
3. Wu Y, Guo Y, Ma Y, Yu H, Wang Z. Small Molecule Inhibitors against the Bacterial Pathogen Brucella. Current Medicinal Chemistry. 2024.
4. Jagadish PS, Jain A, Chandrappa KG, Srinivasa C, Prasad A, Shreevatsa B, Pradeep S, Dharmashekara C, Kollur SP, Shivamallu C. In silico Analysis of Antibacterial Activity of Eclipta alba against *Brucella melitensis*: A Bioinformatics Approach.
5. Bui TB, Nguyen CQ, De Tran Q. Docking-Based Virtual Screening for the Discovery of 1, 3, 4-Oxadiazoles as Aminoacyl-tRNA Synthetase Inhibitors. Can Tho University Journal of Science. 2022 Jun 27;14(2):83-92.
6. López-López E, Cerda-García-Rojas CM, Medina-Franco JL. Consensus Virtual Screening Protocol Towards the Identification of Small Molecules Interacting with the Colchicine Binding Site of the Tubulin-microtubule System. Molecular Informatics. 2023 Jan;42(1):2200166.
7. Yang J, Cai Y, Zhao K, Xie H, Chen X. Concepts and applications of chemical fingerprint for hit and lead screening. Drug Discovery Today. 2022 Sep 13:103356.
8. Bragina, ME., Daina, A., Perez, MAS., Michielin, O. &Zoete, V. SwissSimilarity 2021 Web Tool: Novel Chemical Libraries

and Additional Methods for an Enhanced Ligand-Based Virtual Screening Experience., *Int. J. Mol. Sci,* 2022, *23(2)*, 811.
9. Zoete, V., Daina, A., Bovigny, C., &Michielin, O. SwissSimilarity: A Web Tool for Low to Ultra High Throughput Ligand-Based Virtual Screening., *J. Chem. Inf. Model.,* 2016, *56(8)*, 1399.
10. Joosten RP, Long F, Murshudov GN, Perrakis A. The PDB_ REDO server for macromolecular structure model optimization. IUCrJ. 2014 Jul 1;1(4):213-20.
11. Willard L, Ranjan A, Zhang H, Monzavi H, Boyko RF, Sykes BD, Wishart DS. VADAR: a web server for quantitative evaluation of protein structure quality. Nucleic acids research. 2003 Jul 1;31(13):3316-9.
12. Davis IW, Leaver-Fay A, Chen VB, Block JN, Kapral GJ, Wang X, Murray LW, Arendall III WB, Snoeyink J, Richardson JS, Richardson DC. MolProbity: all-atom contacts and structure validation for proteins and nucleic acids. Nucleic acids research. 2007 Jul 1;35(suppl_2):W375-83.
13. Yang Liu, Maximilian Grimm, et al . CB-Dock: a web server for cavity detection-guided protein–ligand blind docking. ActaPharmacologicaSinica, 2019.
14. Xiong G, Wu Z, Yi J, Fu L, Yang Z, Hsieh C, Yin M, Zeng X, Wu C, Lu A, Chen X. ADMETlab 2.0: an integrated online platform for accurate and comprehensive predictions of ADMET properties. Nucleic Acids Research. 2021 Jul 2;49(W1):W5-14.